

# The measurement of energy loss of 150 GeV positive muons in iron with the TILECAL prototype

TILECAL collaboration

(please send comments to R. Leitner  
Nuclear Center, Charles University, Praha, Czech Republic  
e-mail leitner@hp01.troja.mff.cuni.cz)

## 1 Abstract

We have measured the energy loss of 150 GeV muons in the TILECAL prototype [1] in H8 beam of CERN SPS accelerator.

Differential probability  $dP/dv$  for fractional energy loss  $v = \Delta E_\mu/E_\mu$  was measured in the range  $v = 0.01 \div 0.70$  and it was compared with the theoretical predictions for electron-positron pairs and energetic knock-on electrons production and bremsstrahlung.

Total integrated probability of fractional energy loss  $\int_{0.01}^{0.90} (dP/dv)dv$  of 150 GeV muon per one radiation length in iron was measured to be  $(1.59 \pm 0.03_{stat.} \pm 0.03_{syst.}) \cdot 10^{-3}$  in agreement with theoretical prediction  $1.55 \cdot 10^{-3}$ . The agreement was also found in three different intervals of  $v$  where dominant contributions were caused by different processes of energy loss.

## 2 Introduction

The energy of 150 GeV is a typical energy of muons from the decay of heavy Higgs boson via pair of intermediate bosons Z and W. This channel is considered to be the most promising one for the search of Higgs boson in a very wide mass range.

In the ATLAS detector muons will be measured by the muon chambers inside the air core torroidal magnet after passing more than 100 radiation lengths of

electromagnetic and hadron calorimeters. Muons with energy 150  $GeV$  lose their energy by the production of electron positron pairs (this process dominates in the region from 1.5 to 5  $GeV$  of lost energy by muons), energetic knock-on electrons ( $5\div 20 GeV$ ) and gammas from bremsstrahlung (above 20  $GeV$ ). Therefore the measurement of the energy loss in the whole range 1.5 $\div$ 150  $GeV$  can check all the three processes of loss separately.

Energy losses of high energy muons were measured in cosmic rays experiments [2], [3] and recently also in accelerator experiments [4], [5].

Measurements [2] used Kiel spectrograph to measure the energy of muons, however limited acceptance of the experiment resulted in a low statistics. On the contrary, the measurement [3] had large statistics but the energy of muons was not measured and the spectrum of energy loss extended only up to 0.2 of fractional energy loss and was dominated mainly by the pair production.

Accelerator experiment [4] found their data to be in a good agreement with calculations done by Lohmann et al. [6] based on Kel'ner and Kotov [7] formula for pair production and Petrukhin and Shestakov [10] expressions for bremsstrahlung. The measurements of EMC collaboration [5] was done in the region of bremsstrahlung dominance and a good agreement was found with Tsai's [11] description of this process, which was shown by Tannenbaum [12] to differ from Petrukhin and Shestakov description by approximately 20 %. In the same paper of Tannenbaum[12] the lack of measurements in the region of bremsstrahlung dominance (large fractional energy losses) was clearly mentioned.

### 3 The Measurement

The measurement was done with the prototype of TILECAL [1] hadron calorimeter during 1995 test beam period. For the test beam measurement the scintillator detector (muon wall [13]) was placed behind the calorimeter and another one was fixed to one side of the TILECAL prototype.

The beam of 150  $GeV$  positive muons was defined by three scintillators and its direction was measured by two two-coordinate drift chambers. The beam entered the calorimeter in the middle of central module at theta angle 90 degrees. At this configuration, the TILECAL prototype is a very good electromagnetic calorimeter with active scintillator plate after each 14 mm ( $0.8 X_0$ ) of iron absorber and it is longitudinally segmented into five rows ( $8.8 X_0$  each), i.e. total thickness of the calorimeter at this configuration is about  $44 X_0$ . Total statistics used at present analysis was 100 thousands events.

We have selected events with maximal response in the 2nd or 3rd rows (seen by the beam) of the calorimeter to ensure full containment of electromagnetic showers

produced by electron positron pairs, knock-on electrons or by emitted gammas. Acceptance calculations showed that by this selection we have accepted all showers starting within two rows ( $17.6 X_0$ ) inside the TILECAL prototype. A weak decrease of the acceptance for the energies above 90 GeV (maximal difference is 3%) is due to logarithmic prolongation of electromagnetic showers length and is well described by the formula for the length  $L_{acc.}$ , where accepted showers started:

$$L_{acc.}(E_{shower}) = (17.6 - \ln(E_{shower}(GeV)/90.GeV))X_0 \text{ (see Fig.1).}$$

The energy of electromagnetic shower was taken as the sum of signals in two consecutive rows ( $17.6 X_0$ ) for lowest energies around 1.5 GeV up to four consecutive rows ( $35.2 X_0$ ) for the highest energies. This method minimized corrections for muon signal ( $e_\mu$ ) in the scintillator plates. These corrections are important for lowest energies and should be subtracted from the energy of the shower( $e_{shower}$ ). To keep the additional signal of muons well separated from the signal of electromagnetic shower on the level

$$e_\mu + 3\sigma_\mu \leq e_{shower} - 3\sigma_{shower},$$

it was accepted 1.5 GeV limit as lower edge of studied interval of the energy loss. The electromagnetic shower of 1.5 GeV in the calorimeter produces about 80 electrons and positrons which are detected in scintillators. Because two rows contain 22 scintillator plates, the additional signal of primary muon in the scintillator is about 30% for the shower with the energy 1.5 GeV. The correction is about 4.5% and 0.6% for 15 GeV and 150 GeV showers respectively.

To suppress events with more than one entering particle we have required the signal in muon wall[13] in front of the calorimeter corresponding to one minimum ionizing particle.

Possible hadron contamination of muon beam was eliminated by cuts imposed on impact point and the divergence of the beam together with the requirement that more than 95% of the signal to be deposited in the central module. The electron contamination of muon beam was negligibly small (mean decay length of muons to electrons is about  $10^6$  m), moreover we found no difference in numbers of showers with the maximum in the 3rd row and in the 2nd row where all possible electron contamination would be concentrated.

Possible systematic errors were estimated 0.3 % in the precision of knowledge of iron absorber thickness. About 1.4 % systematic uncertainty is due to absolute energy scale correspondance to the knowledge of the ADC counts to electromagnetic shower energy conversion coefficient  $6.9 \pm 0.1 pC/GeV$ . The precision of

mean muon energy  $150.0 \pm 0.5 \text{ GeV}$  results in another 0.3% contribution to overall systematic error. Maximal total systematic error was estimated to be equal to linear sum of all three contributions, i.e. 2%.

## 4 Results

In each interval of the fractional energy loss  $v = \Delta E_\mu / E_\mu$  we have calculated the mean value  $\langle v \rangle$  of fractional energy loss and differential probability per one radiation length

$$\Delta P / \Delta v = ((N_i / N_{tot}) / \Delta v_i) \cdot (1 / L_{acc}(\langle v \rangle)),$$

where  $N_i$  is the number of events in  $i$ -th interval,  $N_{tot}$  is the total number of events passing the cuts (about  $85 \cdot 10^3$ ),  $\Delta v_i$  is the width of  $i$ -th interval and  $L_{acc}$  is the accepted length (see Fig.1).

We made a comparison of our results with theoretical predictions.

To describe pair production we have used Kel'ner and Kotov[7] expression for differential probability of muon loss per radiation length:

$$\left( \frac{dP}{dv} \right)_{pair} = C \frac{16}{\pi} Z^2 \alpha^2 \frac{1}{v} F(E_\mu, v) \quad (1)$$

here  $C = X_0 \rho \frac{N_A r_e^2}{A} = 1.185 \cdot 10^{-2}$ ,  $N_A = 6.022 \cdot 10^{23} \text{ mol}^{-1}$  is Avogadro number  $X_0 = 1.76 \text{ cm}$  is radiation length,  $\rho = 7.87 \text{ g cm}^{-3}$  is density,  $A = 55.85 \text{ g mol}^{-1}$  is atomic weight and,  $Z = 26$  is atomic number of iron;  $r_e = 2.818 \cdot 10^{-13} \text{ cm}$  is classical electron radius and  $\alpha = 1/137.036$  is the fine structure constant.

Function  $F(E_\mu, v)$  is tabulated in [7] for lead and sodium for different energies of muons. Our interpolation of Kel'ner and Kotov function  $F(E_\mu, v)$  for 150 GeV muon loss in iron is shown on Fig.2 together with the fit  $\ln F_{Fe}(150., v) = -0.175 \ln^2(v) - 2.748 \ln(v) - 9.736$ , which we used in the calculations.

To describe production of energetic knock-on electrons we used formula of Bhabha [8] given in book of Rossi [9] ( $m_e$  is the electron mass):

$$\left( \frac{dP}{dv} \right)_{knock-on} = C 2\pi Z \left( \frac{m_e}{E_\mu} \right) \frac{1 - v + \frac{v^2}{2}}{v^2} \quad (2)$$

To compare our results with bremsstrahlung we used expression given by Petrukhin and Shestakov[10] and another calculation done by Tsai[11].

The expression of Petrukhin and Shestakov ( $m_\mu$  is muon mass):

$$\left(\frac{dP}{dv}\right)_{\text{bremsstrahlung}}^{PS} = C4Z^2\alpha \left(\frac{m_e}{m_\mu}\right)^2 \frac{1}{v} \left(\frac{4}{3} - \frac{4}{3}v + v^2\right) \Phi^{PS}(\delta) \quad (3)$$

contains screening function:

$$\Phi^{PS}(\delta) = \ln \frac{\frac{2}{3} \frac{189m_\mu}{m_e} Z^{-2/3}}{1 + \frac{189\sqrt{e}}{m_e} \delta Z^{-1/3}} \quad (4)$$

where  $\delta = m_\mu^2 v / 2E_\mu(1-v)$  is minimal momentum transfer to the nucleus and  $e = 2.718$ .  $\Phi^{PS}(\delta)$  is an approximation of exact screening function calculations, which is valid within 1% up to  $\delta=0.1m_\mu$  ( $v=0.9$  for  $E_\mu=150GeV$ )[10].

To compare previous formula with differential probability distribution given by Tsai[11] [12] we rewrite Tsai's formula in the form:

$$\left(\frac{dP}{dv}\right)_{\text{bremsstrahlung}}^{TS} = C4Z^2\alpha \left(\frac{m_e}{m_\mu}\right)^2 \frac{1}{v} \left(\frac{4}{3} - \frac{4}{3}v + v^2\right) \Phi^{TS}(\delta) \quad (5)$$

where screening function  $\Phi^{TS}(\delta)$  is defined as follows

$$\begin{aligned} \Phi^{TS}(\delta) = & \frac{\phi_1(a\delta)}{4} - \frac{1}{3} \ln Z - f_{\text{coul}} + \frac{1}{Z} \left( \frac{\psi_1(a'\delta)}{4} - \frac{2}{3} \ln Z \right) \\ & + \frac{\frac{2}{3}(1-v)}{\frac{4}{3} - \frac{4}{3}v + v^2} \left( \frac{\phi_1 - \phi_2}{4} + \frac{1}{Z} \frac{\psi_1 - \psi_2}{4} \right) \end{aligned} \quad (6)$$

$\phi_1$  and  $\psi_1$  are functions of arguments  $a\delta$  and  $a'\delta$  where  $a = 184.15/(\sqrt{e}m_e Z^{1/3})$  and  $a' = 1194/(\sqrt{e}m_e Z^{2/3})$  defined for zero momentum transfer

$\phi_1(0) = 4 \ln(\sqrt{e}aZ^{1/3}m_\mu)$ ,  $\psi_1(0) = 4 \ln(\sqrt{e}a'Z^{2/3}m_\mu)$  and for arbitrary  $\delta$ :

$\phi_1(a\delta) = \phi_1(0) - 2 \ln(1 + (a\delta)^2) - 4(a\delta) \arctg(1/a\delta)$ ,

$\psi_1(a'\delta) = \psi_1(0) - 2 \ln(1 + (a'\delta)^2) - 4(a'\delta) \arctg(1/a'\delta)$ .

Asymptotic behavior of  $\phi_2$  and  $\psi_2$ :  $\phi_1(0) - \phi_2(0) = \psi_1(0) - \psi_2(0) = 2/3$  and  $\phi_1 - \phi_2 = \psi_1 - \psi_2 = 0$  for large arguments is fixed by the relations[11]

$\phi_2(a\delta) = \phi_1(a\delta) - (2/3)/(1 + 6.5a\delta + 6(a\delta)^2)$ ,

$\psi_2(a'\delta) = \psi_1(a'\delta) - (2/3)/(1 + 40a'\delta + 400(a'\delta)^2)$ .

Finally  $f_{\text{coul}} = 4.197 \cdot 10^{-2}$  is correction for Coulomb interaction.

Functions  $\Phi^{PS}(\delta)$  and  $\Phi^{TS}(\delta)$  are plotted on Fig.3 together with the values of  $\Phi(\delta)$  extracted from our data.

Photonuclear interactions contribute also to energy loss of muons. The probability is given by following formula [6]

$$\left(\frac{dP}{dv}\right)_{\text{photonuclear}} = C \left(\frac{A\sigma_{\gamma N}(\epsilon)}{\pi r_e^2}\right) \frac{\alpha}{2} v \Gamma(E_\mu, v) \quad (7)$$

where the function  $\Gamma(E_\mu, v)$  is given

$$\begin{aligned} \Gamma(E_\mu, v) &= \frac{3}{4}G(x) \left( \kappa \ln\left(1 + \frac{m_1^2}{t}\right) - \frac{\kappa m_1^2}{m_1^2 + t} - \frac{2m_\mu^2}{t} \right) \\ &+ \frac{1}{4} \left( \kappa \ln\left(1 + \frac{m_2^2}{t}\right) - \frac{2m_\mu^2}{t} \right) \\ &+ \frac{m_\mu^2}{t} \left( \frac{3}{4}G(x) \frac{m_1^2}{m_1^2 + t} + \frac{1}{4} \frac{m_2^2}{t} \ln\left(1 + \frac{t}{m_2^2}\right) \right) \end{aligned} \quad (8)$$

with

$$\begin{aligned} G(x) &= \frac{3}{x^2} \left( \frac{x^2}{2} - 1 + e^{-x}(1+x) \right) \\ x &= 0.00282 A^{1/3} \sigma_{\gamma N}(\Delta E_\mu) \\ \sigma_{\gamma N}(\Delta E_\mu) &= 114.3 + 1.647 \ln^2(0.0213 \Delta E_\mu) \text{microbarns} \\ t &= \frac{m_\mu^2 v^2}{1-v} \\ \kappa &= 1 - \frac{2}{v} - \frac{2}{v^2} \\ m_1^2 &= 0.54 GeV^2 \\ m_2^2 &= 1.80 GeV^2 \end{aligned}$$

The contribution of photonuclear interactions is about 1 % for lowest values of fractional loss  $v$  and about 5 % for the highest  $v$  (see Fig.4), but it is suppressed by our selection criteria which were optimized for electromagnetic secondary products. We estimated the maximal contribution of photonuclear processes to be about 0.5 % and 2 % for lowest and highest values of  $v$  respectively. This values were subtracted from measured values of  $dP/dv$ .

The spectrum of differential probabilities  $dP/dv$  per one radiation length in iron is plotted on Fig.4 together with data uncorrected for muon signal in scintillators.

The values are tabulated in Table 1.

## 5 Conclusions

The data are compared with the above mentioned theoretical calculations of Kel'ner and Kotov for pair production (curve  $P$  in Fig.4), Bhabha formula for knock-on electrons ( $K$ ) and Petrukhin and Shestakov ( $B^{PS}$ ) and Tsai's ( $B^{TS}$ ) calculations for bremsstrahlung process. Our data are in a very good agreement with theoretical calculations (without any free parameters) in the whole range from 0.01 to 0.7 of the fractional energy loss.

Because different processes dominate in different regions of fractional loss we can check the validity of them separately. We have calculated integrated probabilities  $\Delta P = \int_{v_{min}}^{v_{max}} \frac{dP}{dv} dv$  over the whole range of measured  $v$  and also in three different intervals of  $v$ . Three intervals of  $v$  (see Table 2) were chosen in such a way that about 55% contribution to integrated probability in the first interval was due to production of  $e^+e^-$  pairs, in the second interval the dominant contribution 45% was due to knock-on electrons and bremsstrahlung dominated by about 60% contribution in the third interval of  $v$ . Obtained values in all intervals agree within  $1\sigma$  with theoretical predictions for the bremsstrahlung description of Petrukhin and Shestakov. The value of integrated probability  $\Delta P_{P+K+B^{TS}} = 1.44 \cdot 10^{-4}$  in the region  $v = 0.12 \div 0.90$  calculated with Tsai's description of the bremsstrahlung is about  $2.2\sigma$  higher than the measured value  $\Delta P = (1.18 \pm 0.09_{stat} \pm 0.02_{syst}) \cdot 10^{-4}$ . We can conclude that under the assumption of absolute precision of the description of pair production and knock-on electrons in the region of high  $v$  by the formulae (1) and (2) our data slightly prefer Petrukhin and Shestakov calculations of the bremsstrahlung.

## 6 Acknowledgements

...

Financial support of Prague group by grant GACR/202/93/0532 from Grant Agency of the Czech Republic is acknowledged.

...

## References

- [1] F.Arztizabal et al., NIM A349(1994) 384.
- [2] O.C.Allkofer et al., Phys. Rev. D4(1971) 638.
- [3] K.Mitsui et al., Nuovo Cim. 73A(1983) 1983.
- [4] R.Kopp et al., Z.Phys. C (1985) 171.
- [5] J.J.Aubert et al., Z.Phys. C10(1981) 101.
- [6] W.Lohmann et al., CERN Report 85-03 (1985).
- [7] S.R.Kel'ner and Yu.D.Kotov, Yad. Fiz. 7(1968) 360.
- [8] H.J.Bhabha, Proc. Roy. Soc. A164(1938) 257.
- [9] B.Rossi, High Energy Particles, New York, 1952.
- [10] A.A.Petrukhin and V.V.Shestakov, Can. J. Phys. 46(1968) S377.
- [11] Y.Tsai, Rev. Mod. Phys. 46(1974) 815.
- [12] M.J.Tannenbaum, CERN-PPE/91-134 (1991).
- [13] M.Lokajicek et al., TILECAL-NO-xxx (1995) in preparation.

| $\langle v \rangle$             | $\Delta P/\Delta v$             | $(dP/dv)_{P+K+B^{PS}}$ | $(dP/dv)_{P+K+B^{TS}}$ |
|---------------------------------|---------------------------------|------------------------|------------------------|
| $(1.08 \pm 0.05) \cdot 10^{-2}$ | $(1.53 \pm 0.08) \cdot 10^{-1}$ | $1.45 \cdot 10^{-1}$   | $1.46 \cdot 10^{-1}$   |
| $(1.25 \pm 0.05) \cdot 10^{-2}$ | $(1.10 \pm 0.07) \cdot 10^{-1}$ | $1.07 \cdot 10^{-1}$   | $1.08 \cdot 10^{-1}$   |
| $(1.48 \pm 0.09) \cdot 10^{-2}$ | $(7.4 \pm 0.4) \cdot 10^{-2}$   | $7.47 \cdot 10^{-2}$   | $7.56 \cdot 10^{-2}$   |
| $(1.8 \pm 0.1) \cdot 10^{-2}$   | $(5.4 \pm 0.3) \cdot 10^{-2}$   | $4.83 \cdot 10^{-2}$   | $4.90 \cdot 10^{-2}$   |
| $(2.3 \pm 0.2) \cdot 10^{-2}$   | $(2.7 \pm 0.2) \cdot 10^{-2}$   | $2.95 \cdot 10^{-2}$   | $3.01 \cdot 10^{-2}$   |
| $(3.0 \pm 0.2) \cdot 10^{-2}$   | $(1.8 \pm 0.1) \cdot 10^{-2}$   | $1.70 \cdot 10^{-2}$   | $1.75 \cdot 10^{-2}$   |
| $(3.8 \pm 0.3) \cdot 10^{-2}$   | $(8.6 \pm 0.8) \cdot 10^{-3}$   | $10.1 \cdot 10^{-3}$   | $10.4 \cdot 10^{-3}$   |
| $(4.8 \pm 0.3) \cdot 10^{-2}$   | $(6.7 \pm 0.7) \cdot 10^{-3}$   | $6.03 \cdot 10^{-3}$   | $6.33 \cdot 10^{-3}$   |
| $(5.9 \pm 0.4) \cdot 10^{-2}$   | $(4.1 \pm 0.5) \cdot 10^{-3}$   | $3.92 \cdot 10^{-3}$   | $4.17 \cdot 10^{-3}$   |
| $(7.3 \pm 0.4) \cdot 10^{-2}$   | $(3.2 \pm 0.4) \cdot 10^{-3}$   | $2.53 \cdot 10^{-3}$   | $2.73 \cdot 10^{-3}$   |
| $(8.9 \pm 0.5) \cdot 10^{-2}$   | $(1.6 \pm 0.2) \cdot 10^{-3}$   | $1.71 \cdot 10^{-3}$   | $1.88 \cdot 10^{-3}$   |
| $(1.11 \pm 0.06) \cdot 10^{-1}$ | $(1.1 \pm 0.2) \cdot 10^{-3}$   | $1.12 \cdot 10^{-3}$   | $1.25 \cdot 10^{-3}$   |
| $(1.4 \pm 0.1) \cdot 10^{-1}$   | $(7.7 \pm 1.2) \cdot 10^{-4}$   | $7.31 \cdot 10^{-4}$   | $8.38 \cdot 10^{-4}$   |
| $(1.8 \pm 0.1) \cdot 10^{-1}$   | $(4.9 \pm 0.9) \cdot 10^{-4}$   | $4.74 \cdot 10^{-4}$   | $5.57 \cdot 10^{-4}$   |
| $(2.3 \pm 0.2) \cdot 10^{-1}$   | $(3.4 \pm 0.7) \cdot 10^{-4}$   | $3.06 \cdot 10^{-4}$   | $3.71 \cdot 10^{-4}$   |
| $(3.3 \pm 0.4) \cdot 10^{-1}$   | $(1.4 \pm 0.2) \cdot 10^{-4}$   | $1.60 \cdot 10^{-4}$   | $2.02 \cdot 10^{-4}$   |
| $(5.1 \pm 0.3) \cdot 10^{-1}$   | $(7.5 \pm 2.1) \cdot 10^{-5}$   | $7.43 \cdot 10^{-5}$   | $9.89 \cdot 10^{-5}$   |
| $(7.0 \pm 0.7) \cdot 10^{-1}$   | $(4.0 \pm 0.9) \cdot 10^{-5}$   | $4.26 \cdot 10^{-5}$   | $5.96 \cdot 10^{-5}$   |

Table 1. Comparison of measured values of differential probabilities  $\Delta P/\Delta v$  in the range  $0.01 \div 0.70$  of fractional energy loss with theoretical calculations  $(dP/dv)_{P+K+B^{PS}}$  according to sum of formulae (1), (2) and (3) and  $(dP/dv)_{P+K+B^{TS}}$  according to sum of formulae (1), (2) and (5) in the text. Overall systematic errors of 2% are not quoted.

| $(v_{min}, v_{max})$ | $\Delta P_{measured}$           | $\Delta P_{P+K+B^{PS}}$ | $\Delta P_{P+K+B^{TS}}$ |
|----------------------|---------------------------------|-------------------------|-------------------------|
| (0.01, 0.03)         | $(1.16 \pm 0.03) \cdot 10^{-3}$ | $1.13 \cdot 10^{-3}$    | $1.15 \cdot 10^{-3}$    |
| (0.03, 0.12)         | $(3.06 \pm 0.15) \cdot 10^{-4}$ | $3.04 \cdot 10^{-4}$    | $3.22 \cdot 10^{-4}$    |
| (0.12, 0.90)         | $(1.18 \pm 0.09) \cdot 10^{-4}$ | $1.17 \cdot 10^{-4}$    | $1.44 \cdot 10^{-4}$    |
| (0.01, 0.90)         | $(1.59 \pm 0.03) \cdot 10^{-3}$ | $1.55 \cdot 10^{-3}$    | $1.62 \cdot 10^{-3}$    |

Table 2. Integrated probabilities  $\Delta P = \int_{v_{min}}^{v_{max}} \frac{dP}{dv} dv$  per one radiation length measured in three different intervals  $(v_{min}, v_{max})$  and compared with theoretical calculations for the sum of pair production ( $P$ ), knock-on electrons production ( $K$ ) and two different formulae of the bremsstrahlung ( $B^{PS}$ ) and ( $B^{TS}$ ) (see formulae (1),(2),(3) and (5) respectively). Overall systematic errors of 2% are not quoted.

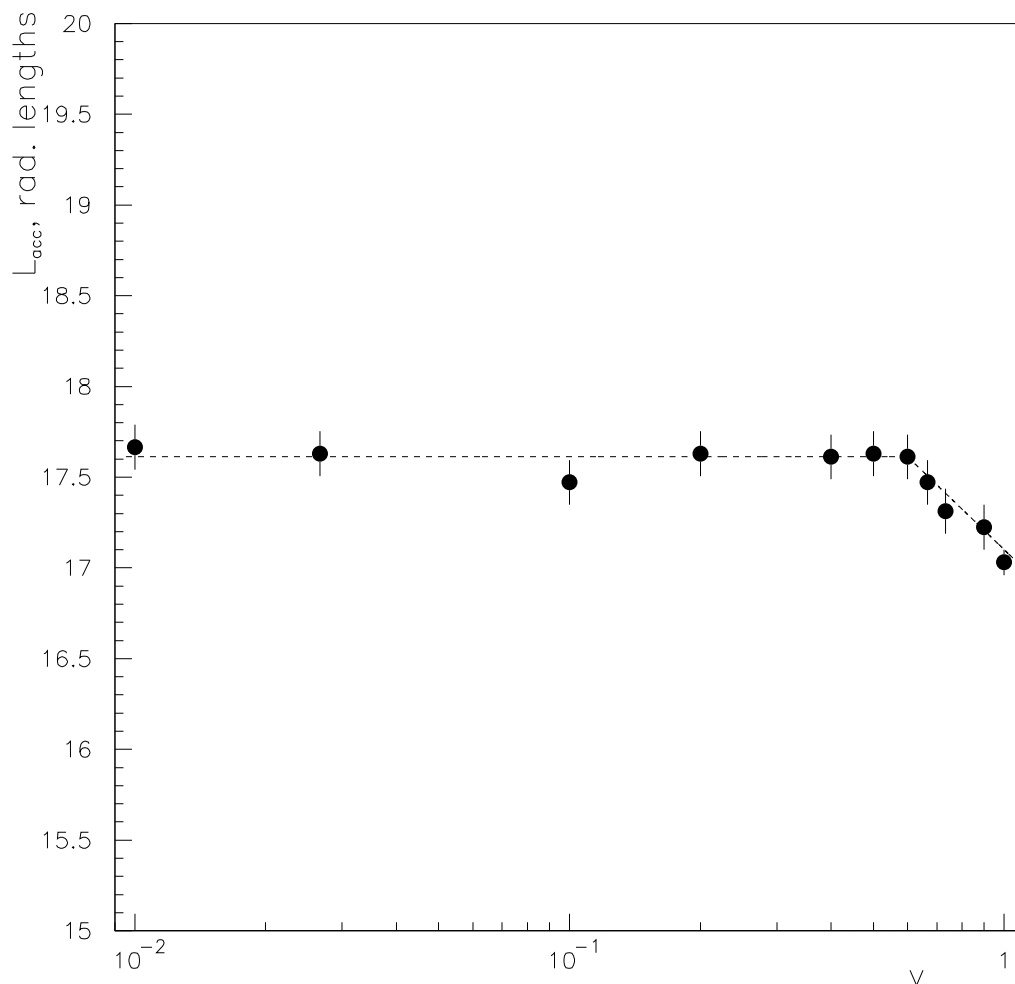


Figure 1:

Length  $L_{acc}$  (in radiation lengths of iron) of the region where accepted showers started is plotted as function of shower energy. The curve is a constant equal to  $17.6 X_0$  for energies up to  $90 \text{ GeV}$  and it falls down according to formula  $L_{acc.}(E_{shower}) = (17.6 - \ln(E_{shower}(\text{GeV})/90.\text{GeV}))X_0$  for energies above  $90 \text{ GeV}$ .

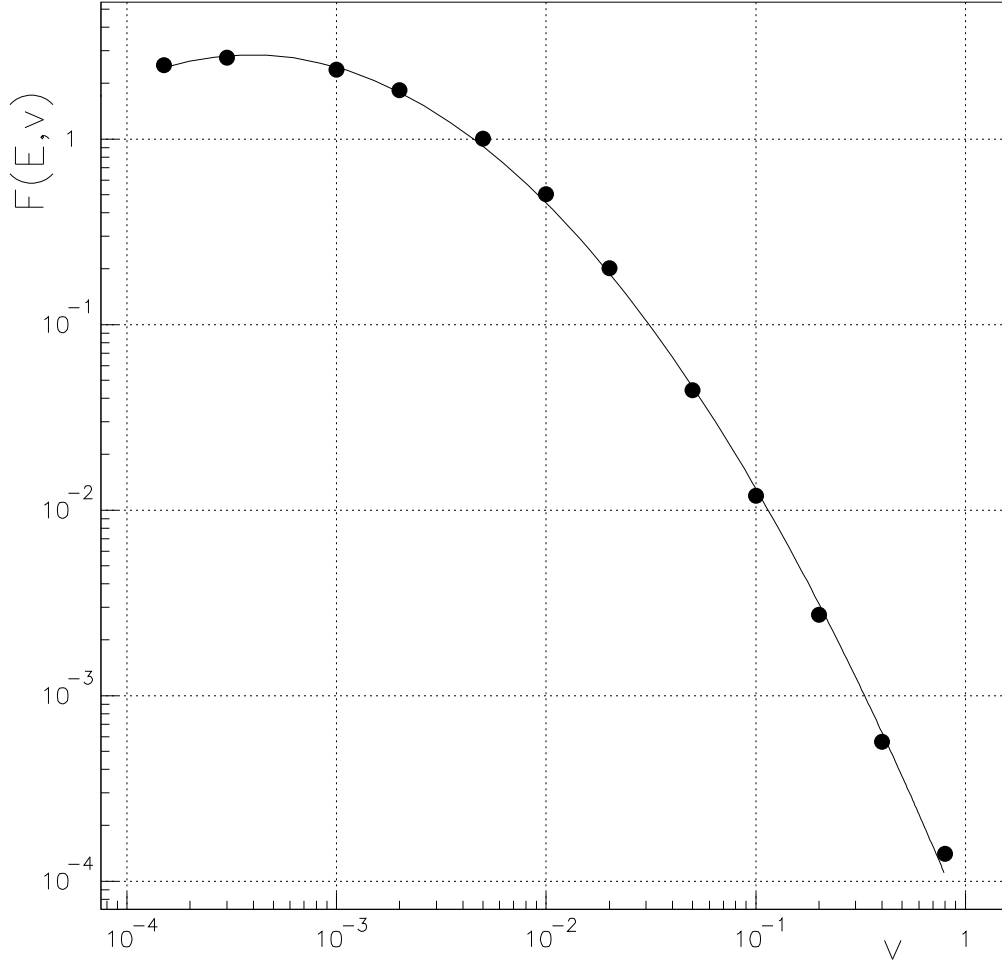


Figure 2:

The function  $F(E_\mu, v)$  (see formula (1) in the text) for  $e^+e^-$  pairs production by 150 GeV muons in iron. The curve corresponds to the fit  $\ln F_{Fe}(150., v) = -0.175 \ln^2(v) - 2.748 \ln(v) - 9.736$ .

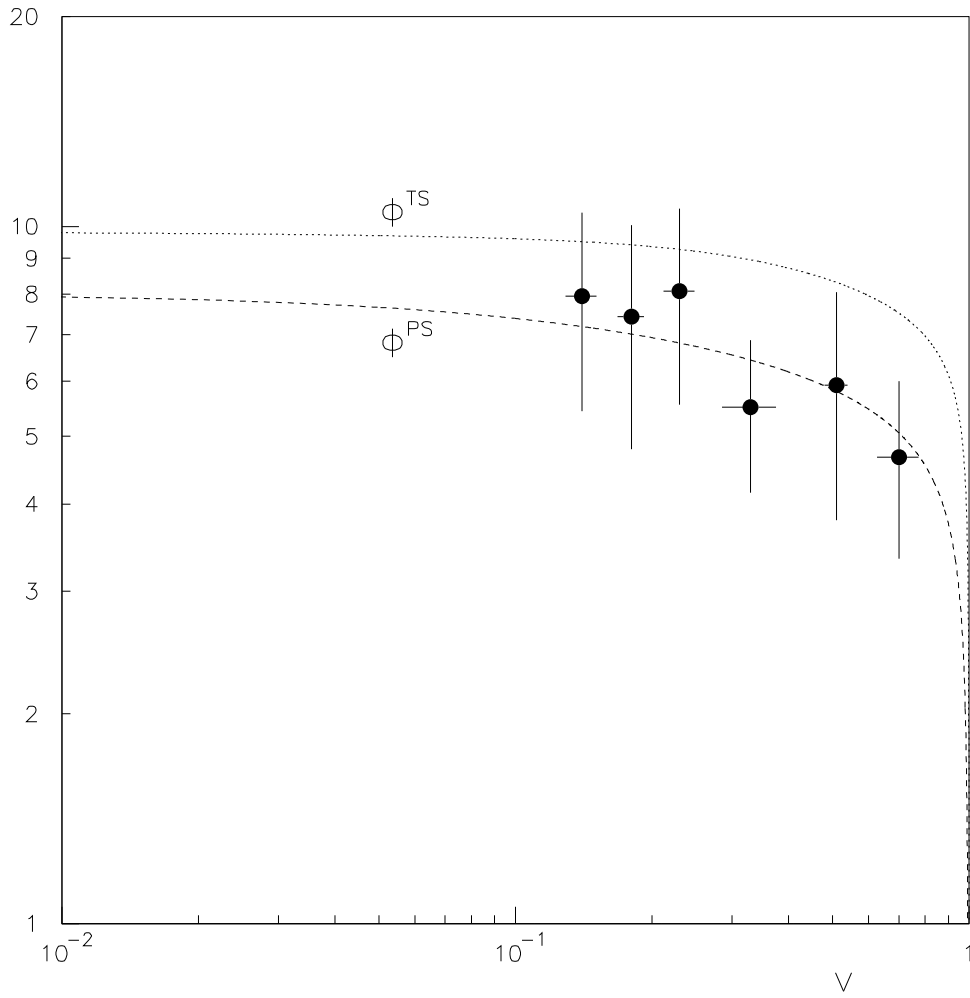


Figure 3:

Comparison of screening functions of Petrukhin and Shestakov  $\Phi^{PS}$  and Tsai's  $\Phi^{TS}$  description of bremsstrahlung of 150 GeV muons in iron. The data points were calculated with the assumption of validity of formulae (1) and (2) for  $e^-e^+$  pairs and knock-on electrons production also in the region of high values of  $\nu$ .

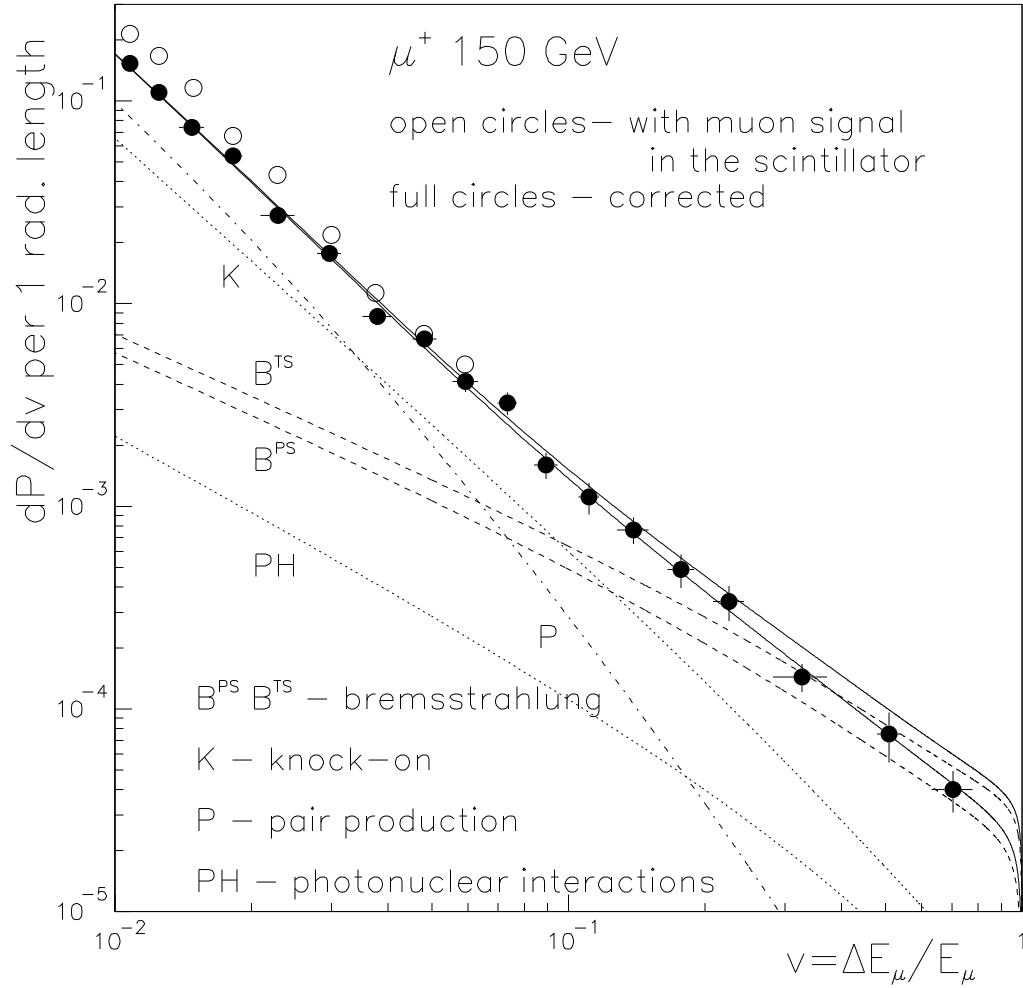


Figure 4:

The distribution of differential probability  $dP/dv$  for energy loss of 150 GeV muons in iron. The curves  $P$ ,  $K$  and  $B^{PS}$ ,  $B^{TS}$  for pair production, knock-on electrons production and bremsstrahlung correspond to eq. (1), (2) and (3),(5) in the text. Full curves are sums of  $P$ ,  $K$ ,  $B^{PS}$  (lower one) and  $P$ ,  $K$ ,  $B^{TS}$  (upper one). The contribution of energy loss due to photonuclear reactions (curve  $PH$ ) is also shown.